



## CAPACITY PARAMETRIC MODEL AND DAMAGE INDEX FOR STEEL BUILDINGS. A PROBABILISTIC APPROACH

S.A. Diaz <sup>(1)</sup>, L.G. Pujades <sup>(2)</sup>, A.H. Barbat <sup>(3)</sup>, J.R. González-Drigo <sup>(4)</sup>, D.A. Hidalgo-Leiva <sup>(5)</sup>

<sup>(1)</sup> Professor, Universidad Juarez Autonoma de Tabasco (UJAT), México. Now at: PhD candidate, DECA-ETCG, UPC Barcelona Tech, Spain. [sergio.alberto.diaz@upc.edu](mailto:sergio.alberto.diaz@upc.edu)

<sup>(2)</sup> Professor, Polytechnic University of Catalonia (UPC). DECA-ETCG. Barcelona Tech, Spain. [lluis.pujades@upc.edu](mailto:lluis.pujades@upc.edu)

<sup>(3)</sup> Professor, Polytechnic University of Catalonia (UPC). DECA-MMCE. Barcelona Tech, Spain. [alex.barbat@upc.edu](mailto:alex.barbat@upc.edu)

<sup>(4)</sup> Professor, Polytechnic University of Catalonia (UPC). EUETIB (CEIB). Barcelona Tech, Spain. [jose.ramon.gonzalez@upc.edu](mailto:jose.ramon.gonzalez@upc.edu)

<sup>(5)</sup> PhD candidate, DECA-ETCG, UPC Barcelona Tech, Spain. [diego.hidalgo@upc.edu](mailto:diego.hidalgo@upc.edu)

### **Abstract**

The capacity and expected seismic damage of several types of steel buildings are assessed. Nonlinear static structural analysis and incremental dynamic analysis (IDA) by means of a probabilistic approach with Monte Carlo Simulation are used. For static analysis, an important contribution of this paper is to extend the parametric models and damage index that were previously proposed for reinforced concrete buildings to steel buildings. Thus, the parametric model is used to fit capacity curves and the expected damage is assessed by means of this new damage index. In this parametric model, the linear and non-linear parts of the capacity curve are separated. The linear part is defined by the initial stiffness and the non-linear part can be parameterized by the integral of a cumulative lognormal function; the ultimate capacity point provides the two last parameters of the five ones that fully define this new capacity model. The damage index is defined as a combination of the energy dissipation and the tangent stiffness degradation. The analyzed buildings are typical of Mexico City and the seismic actions are selected so that they are compatible with the design spectra provided in the seismic code. The results show that, on average, the Park-Ang index, calculated by the IDA, is well fitted by the combination of the contributions to damage index of the stiffness degradation (66-71%) and the one of the energy loss (29-34%); with the advantage that this index can be obtained in an easy, fast and straightforward way from capacity curves. The obtained results show that the parametric model and the damage index are powerful tools for probabilistic assessments of seismic risk.

*Keywords: nonlinear structural analysis; parametric model; Monte Carlo simulation; steel buildings; damage assessment.*

## 1. Introduction

Estimation of seismic vulnerability and risk of structures must take into consideration that the involved variables have high uncertainties. These uncertainties may be organized into two categories, the aleatory (or random) uncertainties and the epistemic (or knowledge) uncertainties [1,2]. Epistemic uncertainties result from lack of knowledge some model or parameter; aleatory uncertainty is inherent in random phenomena. Concerning seismic actions, aleatory uncertainties are associated to the expected ground motions, and therefore cannot be controlled but, certainly, they can be estimated and addressed through probabilistic approaches. Concerning structures, aleatory uncertainties are due to unawareness of its precise mechanical and geometrical properties. Because of the nonlinear response of buildings and structures to earthquakes, another important issue, related to uncertainties, is how they propagate, which depends on the performance of their individual elements, as well as on the non-linear relations between inputs and outputs. Uncertainties can be reduced by employing tests to determine the material properties of the structural elements. To take into account for the effect of uncertainties, seismic design standards recommend to perform deterministic calculations, but using values reduced for resistance of materials and increased actions by means of safety factors. However, in non-linear processes it is well known that the confidence levels associated to the response may be different from the ones associated to the input variables [3]. In the last two decades, it has been emphasized the importance of the capacity spectrum method (CSM) for NonLinear Static Analysis (NLSA)[4,5] and of the incremental dynamic analysis (IDA) for NonLinear Dynamic Analysis (NLDA) [6] from a probabilistic perspective [2]. NLDA is assumed to be the most appropriate tool to assess the damage in structures subjected to dynamic actions. When used the CSM, it is necessary to verify that the expected damage is consistent with the results of IDA [7,8]. Both methods, static and dynamic, have been implemented in recent studies, using the Monte Carlo method [3,9,10]. This fact has allowed to obtain an overall view of the expected performance and providing reliable results. However, probabilistic analyses require to perform a significant number of NLDA's and/or NLSA's, entailing a high computational cost; therefore, would be convenient to develop simplified methods allowing to compare the results obtained by using NLSA and NLDA. One option that can be used for this purpose, was proposed by Pujades et al. [11]; in which a parametric model and a damage index were developed for reinforced concrete buildings; both the parametric model and the damage index were checked through probabilistic NLSA's and NLDA's. According to this parametric model, capacity curves are considered to be composed of a linear part and a non-linear part. The linear part is defined by the initial stiffness or, equivalently, by a straight line whose slope ( $m$ ) is defined by the fundamental period of vibration of the building; the normalized non-linear part represents the degradation of the building and can be parameterized by means of the integral of a cumulative lognormal function defined by two parameters ( $\mu$  and  $\sigma$ ). Considering the ultimate capacity point ( $S_{au}$  and  $S_{du}$ ), the capacity model is then completely defined by five independent parameters. Fig. 1 shown an example of the capacity curve defined by five parameters the parametric model. Concerning to the damage index, this was defined as a combination of the energy dissipation and of the degradation of the tangent stiffness, relative to the one corresponding to the ultimate capacity point; both damage functions can be obtained from the normalized nonlinear part of the pushover curve in a straightforward way. This new damage index was defined and calibrated by means of the Park and Ang damage index obtained from the IDA.

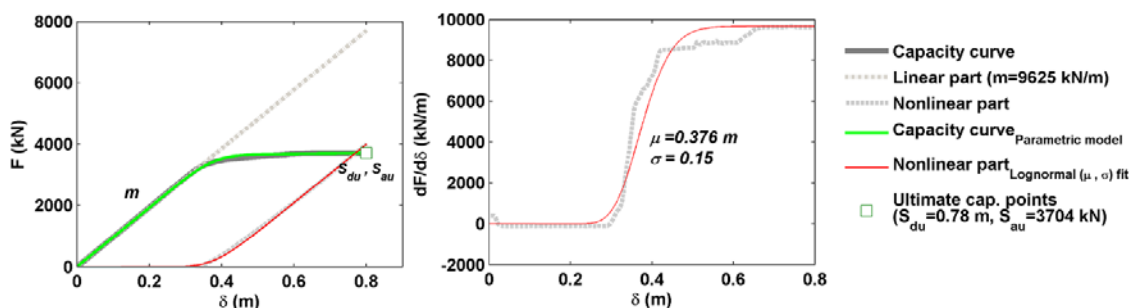


Fig. 1. Capacity curve defined by five independent parameters.

In addition to the fully probabilistic approach to the structural seismic performance of steel buildings, an important contribution of this this article is to check for the parametric and damage models when applied to steel buildings subjected to seismic actions expected in Mexico City; it is worth noting that these models, as proposed in Pujades et al. [11], were tested and used only for reinforced concrete buildings subjected to seismic actions with response spectra compatible with the ones provided in the Eurocode EC-08. Thus, a suite of accelerograms for dynamic analyses has been selected in such a way that their response spectra are compatible with the design spectra recommended for soft soils in this area in the Mexican seismic code [12]. As pointed out above, the analyses, both static and dynamic, are performed by means of a probabilistic approach that uses the Monte Carlo method for sampling and the Latin Hypercube Sampling (LHS) technique to optimize the number of samples. The strength and ductility of beams and columns are considered as random variables; the seismic actions are also considered in a probabilistic way. This fully probabilistic approach allows quantifying the expected uncertainties in the structural responses and induced damage by the uncertainties in the seismic actions and the ones related to the material properties of the structures. The obtained results show how uncertainties increase when the severity of seismic actions increases, as expected. Moreover, it is also shown that the parametric model and the damage index also hold for steel structures, allowing to represent capacity curves by means of a simple model and to analyze the expected damage directly from capacity curves, in a very straightforward way, thus avoiding the large amounts of computations involved on dynamic simulations.

## 2. Mechanical models

Three steel buildings types are analyzed: high-rise (13 story), mid-rise (7 story) and low-rise (3 story) with Special Moment Frames (SMF) configured with W sections (American wide flange section) for beams and columns joined by means of prequalified connections [13] type Fully Restrained (FR). Buildings were designed as office buildings on the basis of the provisions of NTC-DF-2004 [12] and AISC-2010 [14] seismic codes for the México City area. Buildings have rectangular floors, and they have 3 beams of 5 m, in the transversal direction and 4 beams of 6 m in the longitudinal direction (see Fig. 1). Our focus will be on the central frame in the longitudinal direction for each building. The design of the SMFs satisfies the AISC criterion of strong column-weak beam. Fig. 2 sketches the three 2D models (SMF 3, SMF 7 y SMF 13).

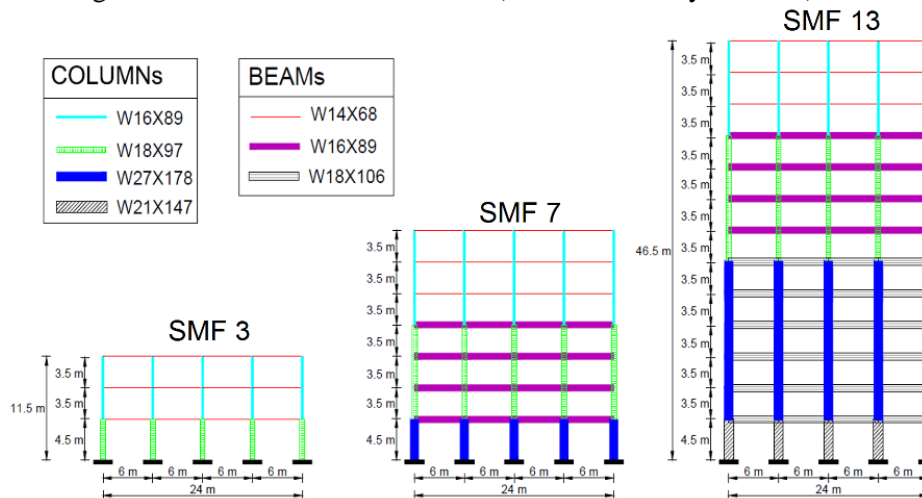


Fig. 2. 2D building models.

NLSAs and NLDA were performed with Ruaumoko 2D [15] software. The weight of the structure, as well as that of the architectural finishes and facilities were considered as dead loads (DL), while the live load (LL) was set according to NTC-DF-2004 [12] for office use. Total gravity load for nonlinear analysis is established as  $1.0DL + 0.2 LL$  [16]. Beams and columns were modeled with FRAME type members, with plastic hinges at their ends. The plastic hinges follow the Bi-Linear Hysteresis rule with hardening and strength reduction based on its ductility factor (see Appendix A - Ruaumoko 2D [15]). Due to limitations of the model adopted, which only reproduces the failure by bending moment and shear force, the interaction between moment and axial force is not considered. In addition, it is expected that most of the damage for this type of buildings is

expected to occur at the ends of the elements, mainly due to the combined effects of moment and shear. Therefore, the interaction of yield surface is defined for columns and beams by the bending moment - angular deformation diagram. Moreover, the values of strength and ductility for the rule of hysteresis were calculated according to the modified Ibarra–Medina–Krawinkler (IMK) model [17,18]; this model establishes strength bounds on the basis of a monotonic backbone curve (Fig. 3a). The backbone curve is defined by three strength parameters [ $M_y$ = effective yield moment,  $M_c$ = capping moment strength (or post-yield strength ratio  $M_c/M_y$ ), and residual moment [ $M_r = \kappa \cdot M_y$ ,  $\kappa=0.4$ ] and four deformation parameters [ $\theta_y$ = yield rotation,  $\theta_p$ = pre-capping plastic rotation for monotonic loading (difference between yield rotation and rotation at maximum moment),  $\theta_{pc}$ = post-capping plastic rotation (difference between rotation at maximum moment and rotation at complete loss of strength), and  $\theta_u$ = ultimate rotation capacity] [18]. The columns of the moment-resisting bays were assumed to be fixed at their bases. P–Delta effects were also considered. The panel zones were modeled in a simplified way by the rotational stiffness in the connections, obtained according to the model proposed by Krawinkler [19] and presented in FEMA 355C [20], and it was input into the model as flexibility at the ends of the beam. In all cases, it was assumed a 2% Rayleigh damping (damping recommended for steel structures [21]). The fundamental periods of the models are 0.632 s, 1.22 s and 1.92 s respectively for SMF3, SMF7 and SMF13 buildings.

### 3. Probabilistic variables

For structural models the mass and damping are assumed to be deterministic and only the strength and ductility of structural elements are considered in a probabilistic way. All the strength parameters of the modified IMK model can be obtained from two properties of the sections: plastic modulus,  $Z$ , and expected yield strength,  $f_y$ . In this research only  $f_y$  is considered as a random variable for the LHS simulations with normal distributions. The mean ( $\mu$ ) value, standard deviation ( $\sigma$ ) or coefficient of variation (COV) and the assumed probability distributions are shown in Table 1.

Ductility of structural sections is defined by the deformation parameters  $\theta_y$ ,  $\theta_p$  and  $\theta_{pc}$  of the modified IMK model and, for W sections, they can be determined by means of the multi-variable empirical equations developed by Lignos & Krawinkler [18]. (See the following Eqs. (1) (2) and (3) respectively).

$$\theta_y = M_y/k_o = 1.17Zf_y/EI \quad (1)$$

$$\theta_p = 0.0865 \left(\frac{h}{t_w}\right)^{-0.365} \left(\frac{b_f}{2t_f}\right)^{-0.140} \left(\frac{L}{d}\right)^{0.340} \left(\frac{c_{unit}^1 d}{533}\right)^{-0.721} \left(\frac{c_{unit}^2 f_y}{355}\right)^{-0.721} \quad \sigma_{ln}=0.32 \quad (2)$$

$$\theta_{pc} = 5.63 \left(\frac{h}{t_w}\right)^{-0.565} \left(\frac{b_f}{2t_f}\right)^{-0.800} \left(\frac{c_{unit}^1 d}{533}\right)^{-0.280} \left(\frac{c_{unit}^2 f_y}{355}\right)^{-0.430} \quad \sigma_{ln}=0.25 \quad (3)$$

where  $k_o$  is the initial elastic stiffness;  $E$  is the modulus of elasticity;  $I$  is the inertia;  $c_{unit}^1$  and  $c_{unit}^2$  are coefficients for units conversion;  $h/t_w$  is the ratio of the web depth over thickness;  $L/d$  is the ratio between the span and depth beam;  $b_f/2t_f$  is the width/thickness ratio of the beam flange, and  $\sigma_{ln}$  is the standard deviation assuming a lognormal fit of experimental data. Finally, the ultimate rotation capacity is estimated as  $\theta_u = 1.5(\theta_y + \theta_p)$ , based on the recommendation by PEER/ATC 72-1 [16]. For this study  $\theta_y$  is considered with a dependent variable of  $f_y$ . The mean ( $\mu$ ) values, standard deviations ( $\sigma_{ln}$ ) and function types used for  $\theta_p$  and  $\theta_{pc}$  are shown in Table 1. For the LHS simulations, both normal distributions of  $f_y$  and lognormal distributions of  $\theta_p$  and  $\theta_{pc}$  were truncated at both ends, the lower and upper limits being determined by the mean value  $\pm 2$  times the standard deviation ( $\mu \pm 2\sigma$ ). The purpose of this truncation is to avoid underestimates or overestimates of the capabilities of the elements with samples without physical meaning.

Two types of correlations are considered: intra- and inter-element. The intra-element correlation is given by the relation between the three parameters simulated for the same hinge; these correlations are derived from Eqs. (2) and (3) [22]. This intra-element correlation is defined in Table 2. On the other hand, the inter-element correlation is attributed to the consistency in workmanship and material quality between different element sections. In research conducted by Idota et al. [23] and Kazantzi et al. [10] it was proposed a value of 0.65 for yield strength of beams and columns of the same production lot. Therefore, based on these researches, an inter-element correlation of 0.65 is proposed for the same type section, and a null correlation is assumed for different sections.

Table 1 – Probabilistic mean of the strength and ductility variables

Type	Variable	Mean ( $\mu$ )	Standard deviation( $\sigma$ )	Function	Upper limit	Lower limit
Strength	$f_y$	375.76 Mpa*	26.68 (COV=0.071*)	Normal distribution	429.14 Mpa	322.4 Mpa
Ductility	$\theta_p$	$\theta_p$ by Ec. 2	$\sigma_{in} = 0.32$	Lognormal distribution	$\theta_p$ by Ec. 2 + 2 $\sigma_{in}$	$\theta_p$ by Ec. 2 - 2 $\sigma_{in}$
Ductility	$\theta_{pc}$	$\theta_{pc}$ by Ec. 3	$\sigma_{in} = 0.25$	Lognormal distribution	$\theta_{pc}$ by Ec. 3 + 2 $\sigma_{in}$	$\theta_{pc}$ by Ec. 3 - 2 $\sigma_{in}$

\* Based on the report by Lignos & Krawinkler [22] for statistics of material yielding strength, obtained from flanges-webs tests for steel A572 grade.

Table 2–Intra-element correlation for random variables of beams and columns.

	$f_y$	$\theta_p$	$\theta_{pc}$
$f_y$	1	0	0
$\theta_p$	0	1	0.69
$\theta_{pc}$	0	0.69	1

To better represent the physical randomness of the problem for each structural element (column or beam), a random sample of the three parameters used ( $f_y$ ,  $\theta_p$  and  $\theta_{pc}$ ) is generated. Then the properties of strength and ductility on the hinges of each element is estimated. It is assumed that hinges at both ends of elements are the same. Thus, the 3-storey model, with 27 elements (15 columns and 12 beams) has 81 random variables; the 7-storey building model with 63 elements (35 columns and 28 beams) has 189 random variables and the 13-storey model with 117 elements (65 columns and 52 beams) has 351 random variables. In order to assess the seismic behavior of these three buildings, with a probabilistic approach, 200 NLSA's and 200 NLDA's are performed for each structural model, resulting a total of 600 NLSA's and 600 NLDA's. It is worth noting that the same structural models are used for both structural analyses, static and dynamic. Fig. 3b shows an example of the modified IMK model used in the structural section (W16x89) of the SMF3 probabilistic models.

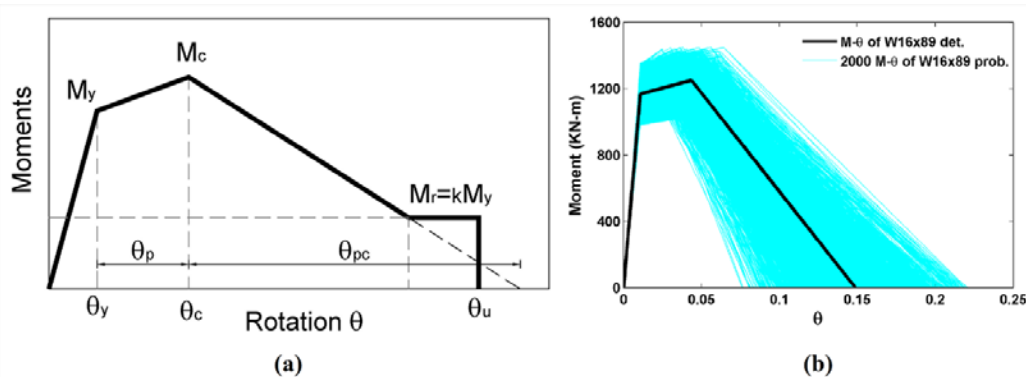


Fig. 3. (a) Modified IMK model: monotonic curve [18]; (b) an example of the modified IMK model used in the structural section (W16x89) of the SMF3 probabilistic models.

#### 4. Probabilistic approach for IDA

To perform IDA, a set of accelerograms representing the characteristics of the study area are needed. The way for obtaining these data set with a probabilistic approach is explained first and the method is then applied to the case of Mexico City. In a first step, a random set of response spectra are generated by means of LHS simulations. The generated response spectra fulfill the following two conditions: i) the mean value is a target spectrum and ii) the standard deviation at each period must be a predefined value. After that and in order to avoid unrealistic -un-correlated response spectra, a new collection of response spectra is obtained by arranging the ordinates of the former spectra at each period. This way, the new sorted spectra also fulfill the required conditions but, they also fulfill the correlation features of actual response spectra. Then, a spectral matching technique, as proposed by Hancock et al. [24], is used to match the response spectrum of a real accelerogram with each one of the simulated spectrum, thus obtaining a set of accelerograms that fulfill the following conditions: i) the mean spectrum matches well the target spectrum, ii) the obtained set of spectra has a predefined standard deviation; and iii) the corresponding accelerograms are representative of the seismic actions expected in the area, that are represented by the selected seed accelerogram. In this study, the design spectrum for the area III<sub>b</sub> of the NTC-DF [12] in Mexico DF has been taken as target spectrum. Moreover, the standard deviation has been set to 1% for periods from 0 to 2 s, corresponding to the range where the periods of the

buildings are located, and 5% for periods greater than 2 s. Concerning to the seed accelerograms, the selection method proposed by Vargas et al. [3] was applied to a database of 2554 accelerograms (three component) recorded in the Mexico City area. This way, four accelerograms with response spectra compatible with the target spectrum were selected. Fig. 4 shows the selected seed accelerogram, the matched ones and the corresponding response spectra. It is worth noting that this large database of Mexican accelerogram was previously analyzed by Diaz et al. [25]. Table 3 shows the characteristics of the selected accelerograms and corresponding earthquakes. For each seed accelerogram, the spectral matching is used to get 5 new accelerograms fulfilling the three probabilistic conditions described above. This way a set of 20 accelerograms were obtained. This number of accelerograms was considered adequate as the Mexican seismic code [12] suggests to use at least four accelerograms; this number of 20 acceleration time histories was also considered suitable to deal with the uncertainties in the seismic actions as they represent well the assumed probabilistic distributions (see Fig. 5). An example of the application of the spectral matching technique for single selected accelerograms is shown in Fig. 4 and the whole set of response spectra corresponding to the 20 compatible accelerograms is shown in Fig. 5. The excellent matching obtained can be observed in both figures.

Table 3– Characteristics of the 4 seed accelerograms selected by of their compatibility with the target spectrum.

Accelerogram	Station	Date	Duration (seg)	Epicenter			Magnitude (Mw)	Component	PGA (cm/s <sup>2</sup> )	Epicentral distance (km)	Azimut Sta-Epi
				Latitude	Longitude	Depth (Km)					
acc1	TH35	20/03/2012	227.47	16.25 N	98.52 W	16	7.4	S00E	49.6	340.58	171.34
acc2	AE02	30/09/1999	383.74	15.95 N	97.03 W	16	7.5	N90W	21.3	442.48	150.64
acc3	PCSE	11/01/1997	209.97	17.91 N	103.04 W	16	6.5	S65W	14.6	442.84	248.35
acc4	DM12	14/09/1995	263.94	16.31 N	98.88 W	22	7.3	N00E	19.3	347.79	176.20

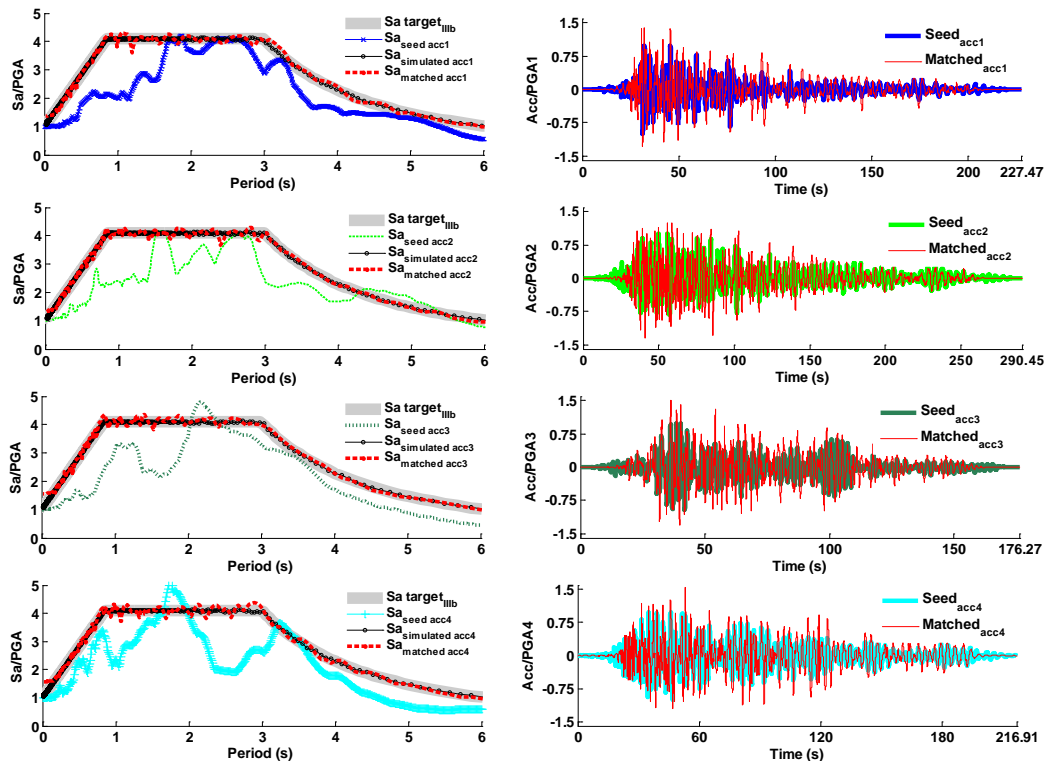


Fig. 4. Target spectrum, and response spectra of the seed and matched accelerograms (right). Seed and matched accelerograms (left).

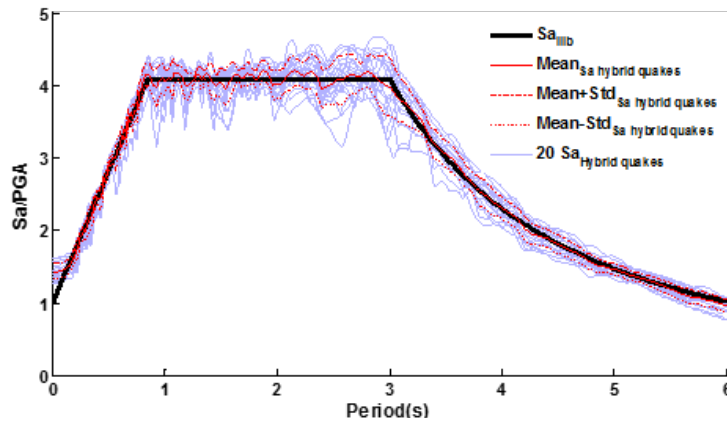


Fig. 5. Response spectra of the 20 accelerograms; mean and standard deviations are also depicted.

## 5. Parametric model

In this section, the parametric model for capacity spectra [11] is applied to steel buildings. The deterministic and probabilistic cases are analyzed. Mean values of strength-ductility of the sections are used for the deterministic approach and, as pointed out above; 600 models generated by LHS are used for the probabilistic approach.

### 5.1. Capacity curves

The capacity curves are obtained by means of an adaptive pushover analysis (PA) [15,26]. Fig. 6 shows these capacity curves. The 50th percentiles (median) match well the deterministic curves for SMF3 and SMF7 models; for SMF13 building and for large displacements, the deterministic curve is a little bit greater than the median one; this fact is attributed to a greater impact of the uncertainties of the mechanical properties in the nonlinear behavior of the structures; note also that SMF13 buildings are high-rise buildings, thus having more structural elements than low-rise and mid-rise buildings. The ultimate displacements ( $D_u$ ) of all the capacity curves show that the deterministic approach is conservative, according to the use of mean values; Table 4 shows the weights and normalized modal participation factors used to transform capacity curves into capacity spectra.

Table 4 – Weights,  $w_i$ , and normalized modal participation factors,  $\Phi_i I$ .

Storey		1	2	3	4	5	6	7	8	9	10	11	12	13
SMF3	$w_i$ (KN)	885.9	881.4	605.6										
	$\Phi_i I$	0.4	0.775	1										
SMF7	$w_i$ (KN)	902.6	890.6	890.6	889.6	881.4	881.4	605.6						
	$\Phi_i I$	0.133	0.313	0.489	0.647	0.803	0.929	1						
SMF13	$w_i$ (KN)	924.5	909.7	909.7	909.7	909.7	903.2	890.6	890.6	890.6	889.6	881.4	881.4	605.6
	$\Phi_i I$	0.057	0.135	0.219	0.303	0.384	0.463	0.563	0.664	0.755	0.832	0.906	0.965	1

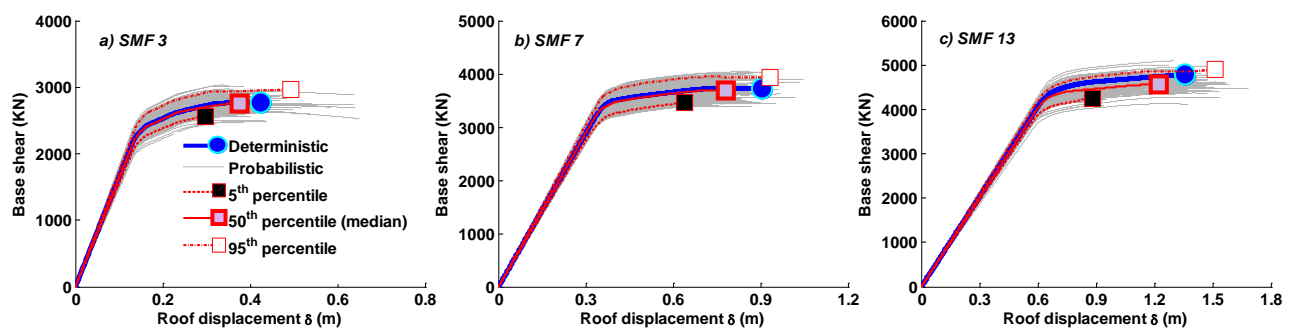


Fig. 6. Deterministic, probabilistic and percentiles of the capacity curves obtained.

### 5.2. Parameters of the capacity model

The parametric model considers that the capacity curve  $F(\delta)$  is composed of a linear part  $F_L(\delta)$  and a nonlinear part  $F_{NL}(\delta)$ , where  $\delta$  is the roof displacement.  $F_L(\delta)$  would be assuming that the building has a linear and elastic

behavior and it is represented by a straight line whose slope ( $m$ ) is defined by the period of the fundamental mode of vibration of the structure. The slope ( $m$ ) is the first parameter of the parametric model.  $F_{NL}(\delta)$  would contain strictly the nonlinear response of the building and can be obtained by subtracting the true capacity curve from the linear curve with Eq. (4).

$$F_{NL}(\delta) = F_L(\delta) - F(\delta) = m\delta - F(\delta) \quad (4)$$

The first derivative of the capacity curve and, indeed, that one of the nonlinear part, is related to the tangent stiffness and to the progressive degradation of the strength of the structure; therefore, the parametric model is based on the fit of the normalized nonlinear part of the capacity curve; the same model is valid for capacity spectra, as it is based on normalized roof displacements and base shears. Fig. 7(top) shows  $F(\delta)$ ,  $F_L(\delta)$  and  $F_{NL}(\delta)$  of the 50<sup>th</sup> percentile (median) of capacity spectra; Fig. 7(bottom) shows the corresponding derivatives:  $dF(\delta)/d\delta$ ,  $dF_{NL}(\delta)/d\delta$  y  $dF_L(\delta)/d\delta = m$ . From Eq. (4) it follows that the function  $dF_L(\delta)/d\delta$  fulfils the equation (5):

$$\frac{d}{d\delta} F_{NL}(\delta) = m - \frac{d}{d\delta} F_L(\delta) \quad (5)$$

The normalized first derivative of the nonlinear part is well represented by a cumulative lognormal function as defined in Eqs. (7) and (8) by the parameters  $\mu$  and  $\sigma$  (note that also a Beta function can be used) [11]. That is, the scaled first derivative  $\Psi'$  and the derivative of this  $\Psi''$  satisfy the following equations:

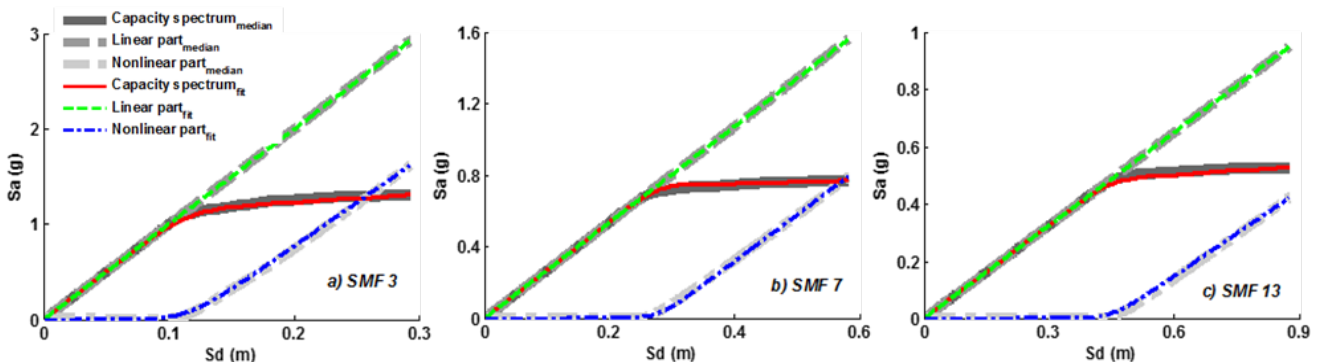
$$\Psi'(A\delta) = B \frac{dF_{NL}(\delta)}{d\delta} \quad 0 \leq A\delta \leq 1 \quad (6)$$

$$\Psi''(A\delta) = \frac{1}{(A\delta)\sigma\sqrt{2\pi}} e^{-\frac{(\ln(A\delta) - \ln(\mu))^2}{2\sigma^2}} \quad 0 \leq A\delta \leq 1 \quad (7)$$

$$\Psi'(A\delta) = \int_0^{A\delta} \Psi''(\xi) d(\xi) \quad 0 \leq A\delta \leq 1 \quad (8)$$

$$F_{NL}(A\delta) = \frac{1}{B} \int_0^{A\delta} \Psi'(\xi) d(\xi) \quad 0 \leq A\delta \leq 1 \quad (9)$$

where  $A$  is  $1/\delta_{max}$  and  $1/B$  is  $1/(m-m^*)$ ;  $m^*$  being the final slope of the capacity curve or the capacity spectrum. Parameters  $\mu$  and  $\sigma$  can then be estimated by means of a least squares fit.  $F_{NL}(A\delta)$ , function allows to determine the two parameters of the model. In addition to  $\mu$  and  $\sigma$ , capacity spectra also depend on the following parameters: i) the slope  $m$  of the linear part; ii) the ultimate spectral displacement,  $S_{du}$ ; and iii) the spectral acceleration,  $S_{au}$ , of the ultimate capacity point. Therefore, a capacity curve (or a capacity spectrum) is entirely defined by the following five independent parameters:  $\mu$ ,  $\sigma$ ,  $m$ ,  $S_{du}$  and  $S_{au}$ . Consequently, families of capacity spectra may have the same lognormal model. The construction of these curves is simple and straightforward undoing the steps explained above (see Eqs. 6 - 9). Fig. 7 summarizes the procedure to obtain the parametric model for a capacity spectrum; results of the target and fitted capacity spectrum together with its first derivative, are shown. The differences are very small and always below 3%. This parametric model has been tested with a significant number of capacity spectra, with excellent results in all the cases (see Fig. 8). The five parameters of deterministic models, probabilistic percentiles and the % mean error between target and fitted are given in Table 5. It is worth noting that this values, may be also useful for probabilistic assessments of seismic risk.



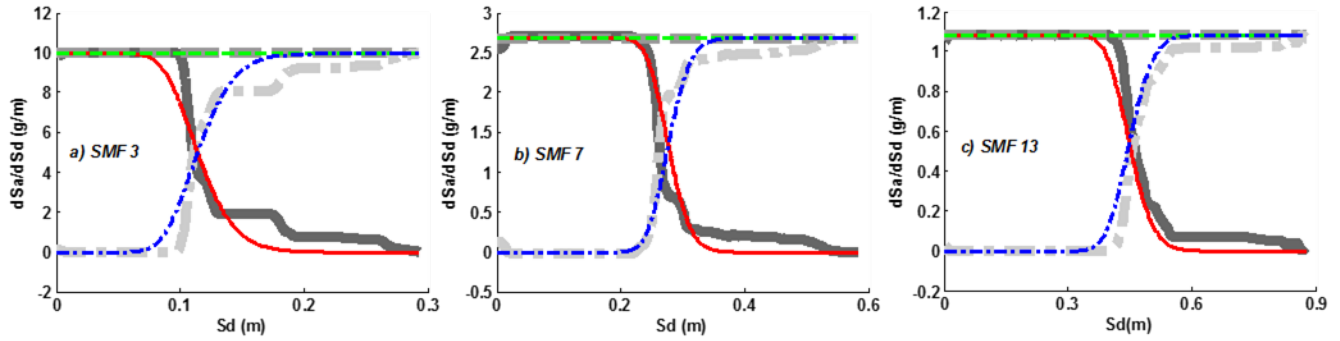


Fig. 7. Linear part, nonlinear part, first derivative and lognormal fits for probabilistic 50<sup>th</sup> percentile (median) of the models a) SMF 3, b) SMF 7 and c) SMF 13.

Table 5 – Parameters of the parametric model for deterministic and probabilistic percentiles of the capacity spectra.

	SMF3						SMF7						SMF13					
	m (g/m)	Sdu (m)	Sau (g)	$\mu$	$\sigma$	%Mean error	m (g/m)	Sdu (m)	Sau (g)	$\mu$	$\sigma$	%Mean error	m (g/m)	Sdu (m)	Sau (g)	$\mu$	$\sigma$	%Mean error
Deterministic	10.05	0.33	1.31	0.37	0.25	0.17	2.70	0.67	0.78	0.40	0.10	0.77	1.10	0.97	0.55	0.49	0.10	0.06
5 <sup>th</sup> percentile	9.44	0.23	1.21	0.48	0.10	0.25	2.55	0.48	0.72	0.58	0.15	0.65	1.04	0.63	0.49	0.70	0.05	0.01
Median	9.96	0.29	1.30	0.39	0.20	1.18	2.68	0.58	0.77	0.48	0.10	0.55	1.08	0.88	0.53	0.51	0.10	0.93
95 <sup>th</sup> percentile	10.67	0.38	1.40	0.30	0.15	2.74	2.84	0.69	0.83	0.39	0.10	0.84	1.12	1.09	0.57	0.46	0.15	1.26

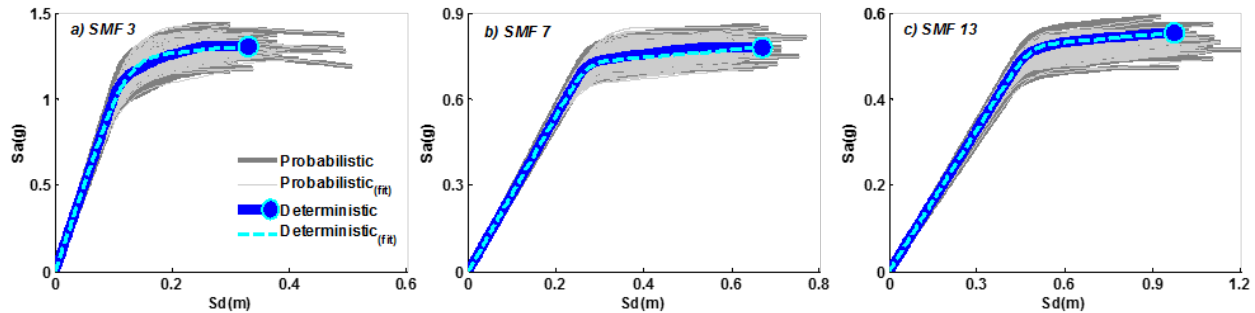


Fig. 8. Capacity spectra target and fitted of the deterministic and probabilistic models of the buildings.

## 6. Damage

The damage index  $DI_{CC}$  as proposed by Pujades et al. [11], is obtained from the capacity curve or capacity spectrum by means of simple and straightforward calculations; and has been calibrated so that it is equivalent to the well-known Park-Ang damage index  $DI_{PA}$ [27].  $DI_{CC}$  is based on the combination of a stiffness degradation function  $K(\delta)$  and an energy dissipation function  $E(\delta)$  relative to the residual stiffness and total energy at the ultimate capacity point.  $E(\delta)$  is easily obtained from the integration of the nonlinear part (Eq. 10).

$$E(\delta) = \int_0^{\delta} F_{NL}(\xi) d(\xi); \quad 0 \leq \delta \leq \delta_u; \quad 0 \leq E(\delta) \leq E(\delta_u) \quad (10)$$

$E(\delta)$  is related to the energy dissipated by the structure when it reaches a displacement  $\delta$ . It is useful to work with the function normalized in abscissae and in ordinates. Thus the following equation can be used

$$E_N(\delta_N) = \frac{E(\delta/\delta_u)}{E(\delta)}; \quad 0 \leq \delta_N \leq 1; \quad 0 \leq E_N(\delta_N) \leq 1 \quad (11)$$

$E_N(\delta_N)$  is the ratio between the energy dissipated as a function of the relative displacement  $\delta_N = \delta/\delta_u$ , and the total energy that the structure has dissipated at the ultimate displacement  $E(\delta_u)$ .

$K(\delta)$  is related to tangent stiffness and it is defined by the following Eq. (12), which also can be transformed into another one varying between 0 and 1 and also can be normalized for displacements  $K_N(\delta_N)$  to Eq. (13)

$$K(\delta) = \frac{\left[ \frac{F(\delta)}{\delta} \right]_{\max} - F(\delta)/\delta}{\left[ \frac{F(\delta)}{\delta} \right]_{\max} - \left[ \frac{F(\delta)}{\delta} \right]_{\min}}; \quad 0 \leq \delta \leq \delta_u; \quad 0 \leq K(\delta) \leq 1 \quad (12)$$

$$K_N(\delta_N) = K\left(\frac{\delta}{\delta_u}\right); \quad 0 \leq \delta_N \leq 1; \quad 0 \leq K_N(\delta_N) \leq 1 \quad (13)$$

$K_N(\delta_N)$  is the ratio between the stiffness variation with respect to the maximum, and the total variation of stiffness.

The damage index  $DI_{CC}(\delta_N)$  is defined by the following two equations

$$DI_{CC}(\delta_N) = \alpha K_{NN}(\delta_N) + (1 - \alpha) E_{NN}(\delta_N) \cong DI_{PA} \quad (14)$$

Where

$$K_{NN}(\delta_N) = DI_{PA}(\delta_u) K_N(\delta_N), \quad E_{NN}(\delta_N) = DI_{PA}(\delta_u) E_N(\delta_N) \quad \text{and for } \delta_N = 1, \quad (15)$$

Thus,  $DI_{PA}$  can be used to calibrate the value of the parameter  $\alpha$ .  $DI_{CC}(\delta_N)$  is calculated from the capacity curves analyzed and calibrated by respective  $DI_{PA}$  of IDA. For the Probabilistic IDA's the set of 20 matched accelerograms has been used; where is selected one for each model with a uniformly random distribution. For the deterministic IDAs the four matched accelerograms shown in Fig. 4, are used and the mean value is obtained. The roof displacements  $\delta$ - $DI_{PA}$  for models are shown in Fig. 9. Observe that deterministic  $DI_{PA}$ 's are conservative compared with probabilistic 50<sup>th</sup> percentile (median); similar behavior has been observed for the capacity curves.

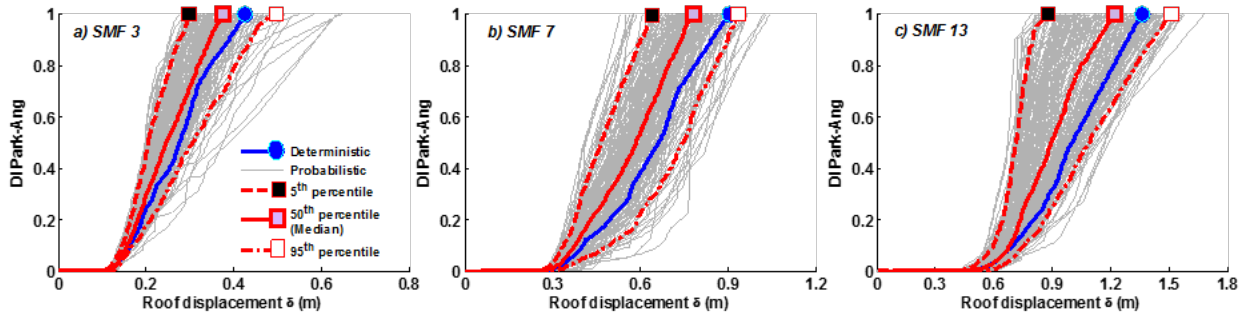


Fig. 9. Roof displacement ( $\delta$ )- $DI_{PA}$  by IDA's of the models a) SMF 3, b) SMF 7 and c) SMF 13.

The functions of tangent stiffness,  $K_{NN}(\delta_N)$ , Energy,  $E_{NN}(\delta_N)$  and damage  $DI_{CC}(\delta_N)$  obtained from of the median capacity curve are shown in Fig. 10.  $DI_{CC}(\delta_N)$  has been calibrated by using the  $DI_{PA}$  (median). The parameter  $\alpha$ , was obtained by means of a least squares fit of Eq. (14). The value of  $\alpha$  is directly related to the percentage of contribution to damage of the stiffness degradation, while their complement in the Eq. 14 corresponds to the contribution of the energy dissipation. For the cases discussed here,  $\alpha$  varies between 0.66 and 0.71. Damage indices  $ID_{CC}$  obtained for deterministic and percentiles capacity curves and the corresponding  $ID_{PA}$  are shown in Fig. 11.  $\alpha$  values are 0.71, 0.66 and 0.67 for SMF3, SMF7 and SMF13 respectively; it is a similar range to the one obtained for the  $ID_{CC}$  (median) and similar range was also reported by Pujades et al. [11] for reinforced concrete buildings. In conclusion, The Park and Ang damage index  $DI_{PA}$ (median) based on dynamic analysis is well represented by the new damage index  $DI_{CC}$ (median) obtained directly from capacity curves. In this case the contributions to damage of the stiffness degradation are in the range 66-71%, while the a one of the energy loss in the range 29-34%.

## 7. Summary and discussion

In this paper it is presented a probabilistic approach allowing quantifying the uncertainties on the seismic response and performance of buildings produced by uncertainties on their mechanical properties (strength and ductility) and on the seismic actions. Concerning seismic actions they are selected according to the seismic hazard of the Mexico City area; thus, four accelerograms recorded in this area have been selected an modified to match the design response spectra provided by the Mexican code for the area; moreover a set of 20

accelerograms have been also obtained by means of spectral matching techniques allowing to obtain 20 accelerograms with predefined mean values and standard deviations, thus providing acceleration time histories compatible with predefined design spectra and predefined dispersion. The procedure is applied to high-rise (13 story), mid-rise (7 story) and low-rise (3 story) steel buildings with Special Moment Frames (SMF); Deterministic and probabilistic NLSA and NLDA have been performed, allowing also the comparison of the deterministic and probabilistic results of both static and dynamic analyses. The main conclusions of this work are as follows. i) The use of mean values in deterministic simplified approaches are conservative; because the obtained expected damage in Fig. 9 and Fig. 11, show that may be lower than the one obtained 50th percentile approach. ii) A recently proposed parametric model and damage index has been implemented for steel buildings. The parametric model allows to define capacity curves by means of five independent parameters. The damage index can be easily obtained from capacity curves, and takes into account the tangent stiffness degradation and the energy loss. This damage index is calibrated with the Park and Ang damage index obtained from dynamic incremental analysis. For the buildings analyzed the contribution to the damage of the stiffness degradation and the one of energy loss are about 70 and 30% respectively. This contribution to damage of the energy dissipation processes is about a 10% higher than the one obtained by Pujades et al. [11] for a reinforced concrete building. This increase on the damage, due to energy dissipation, is attributed to the long duration of the accelerograms used here due to the long epicentral distances of the earthquakes and to the soft soils of the Mexico City study area. Longer durations imply a bigger number of hysteresis cycles for the same spectral displacements, thus increasing the dissipation of energy. iii) Finally, the parametric model and the capacity based damage index have been tested for a large number for steel buildings and seismic actions, with excellent results, thus corroborating their usefulness, simplicity, versatility and robustness. Both, the parametric model and the capacity based damage index, maybe especially useful in probabilistic approaches as they reduce significantly the computation time and provide reliable results.

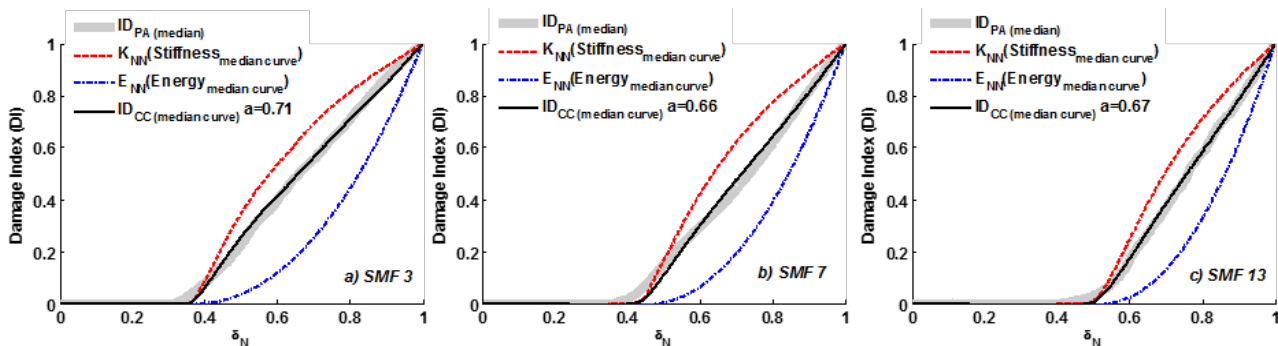


Fig. 10. The energy and stiffness functions and calibration of the  $DI_{CC}(\delta_N)$  from the capacity curve (median) of the models a) SMF 3, b) SMF 7 and c) SMF 13.

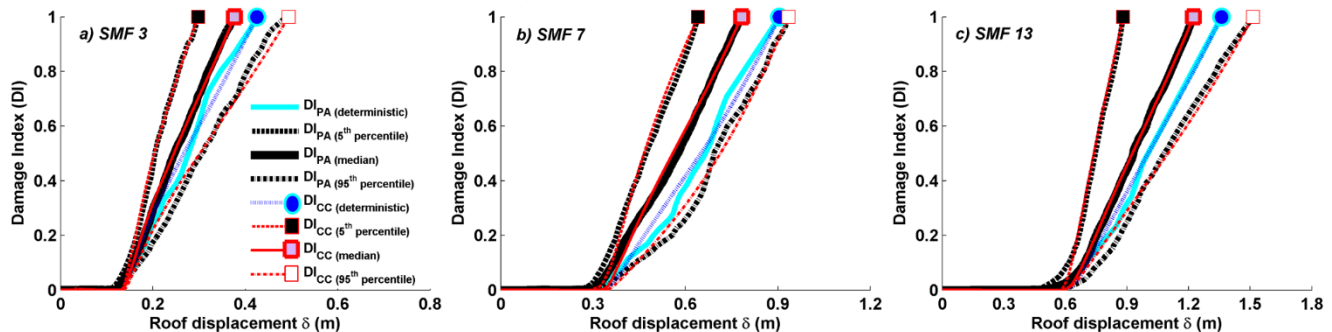


Fig. 11.  $DI_{CC}$  and  $DI_{PA}$  of the deterministic and percentiles models a) SMF 3, b) SMF 7 and c) SMF 13.

## 8. Acknowledgements

This research has been partially funded by the Spanish Government, by the European Commission and with FEDER funds, through the research projects: CGL2011-23621 and CGL2015-65913-P The first author holds a PhD fellowships from the Universidad Juarez Autonoma de Tabasco (UJAT) and from the 'Programa de

Mejoramiento del Profesorado, México (PROMEP)'. Hidalgo-Leiva DA also is the holder of a PhD fellowship from the OAICE the Universidad de Costa Rica (UCR) and CONICIT the Government of Costa Rica.

## 9. References

- [1] Wen YK, Ellingwood BR, Veneziano D, Bracci J (2003): Uncertainty modeling in earthquake engineering. *Technical Report* MAE Center Project FD-2.
- [2] McGuire RK (2004). Seismic hazard and risk analysis. *Earthquake engineering research Institute (EERI)*. Oakland. Ca. 221 pp.
- [3] Vargas YF, Pujades LG, Barbat AH, Hurtado JE (2013): Capacity, fragility and damage in reinforced concrete buildings: A probabilistic approach. *Bulletin of Earthquake Engineering*, **11**(6), 2007-2032.
- [4] Freeman SA (1998): The capacity spectrum method as a tool for seismic design. *Proceedings of the 11<sup>th</sup> European Conference on Earthquake Engineering*, Paris, France.
- [5] ATC-40 (1996): Seismic evaluation and retrofit of concrete buildings. *Technical Report* Applied Technology Council, Redwood City, CA.
- [6] Vamvatsikos D, Cornell CA (2002): Incremental dynamic analysis. *Earthquake Engineering & Structural Dynamics*, **31**(3), 491-514.
- [7] Mwafy A, Elnashai A (2001): Static pushover versus dynamic collapse analysis of RC buildings. *Engineering Structures* **23**(5),407–424.
- [8] Kim SP, Kurama YC (2008): An alternative pushover analysis procedure to estimate seismic displacement demands. *Engineering Structures*,**30**(12),3793–3807.
- [9] Fragiadakis M, Vamvatsikos D (2010) Fast performance uncertainty estimation via pushover and approximate IDA. *Earthq Eng Struct Dyn*, 39: 683-703.
- [10] Kazantzi AK, Vamvatsikos D, Lignos DG (2014): Seismic performance of a steel moment-resisting frame subject to strength and ductility uncertainty. *Engineering Structures*,**78**,69–77.
- [11] Pujades LG, Vargas-Alzate YF, Barbat AH, González-Drigo JR (2015). Parametric model for capacity curves. *Bulletin of Earthquake Engineering*. **13**(5), 1347–1376.
- [12] NTC-DF (2004): Norma tecnica complementaria del Distrito Federal. *Technical Report* Gaceta oficial del Distrito Federal, México.
- [13] ANSI/AISC 358-10 (2010): Prequalified connections for special and intermediate steel moment frames for seismic applications. *Technical Report*: American Institute of Steel Construcción. USA.
- [14] AISC (2010). Specification for structural steel buildings. *Technical Report* American Institute of Steel Construction. USA.
- [15] Carr JA (2002): Ruaumoko 2d and 3d Inelastic Dynamic Analysis. *Computer Program Library*: University of Canterbury.
- [16] PEER/ATC 72-1 (2010): Modeling and acceptance criteria for seismic design and analysis of tall buildings. *Technical Report* Applied Technology Council (ATC) and Pacific Earthquake Engineering Research (PEER), Berkeley, USA.
- [17] Ibarra LF, Medina RA, Krawinkler H (2005): Hysteretic models that incorporate strength and stiffness deterioration. *Earthquake Engineering & Structural Dynamics*, **34**(12), 1489–1511.
- [18] Lignos DG, Krawinkler H (2011): Deterioration modeling of steel components in support of collapse prediction of steel moment frames under earthquake loading. *Journal of Structural Engineering*, **137**(11),1291–1302.
- [19] Krawinkler H (1978): Shear design of steel frame joints. *Engineering Journal AISC*.
- [20] FEMA 355C (2000): State of the art report on system performance of steel moment frames subject to earthquake ground shaking. *Technical Report* SAC Joint Venture Partnership for the Federal Emergency Management Agency. Washington, D.C.
- [21] SAC (1996). Analytical and field investigations of buildings affected by the Northridge earthquake. *Technical Report* No. SAC-95-04, Prepared by SAC Joint Venture, a Partnership of SEAOC, ATC and CUREE.

- [22] Lignos DG, Krawinkler H (2009): Sidesway collapse of deteriorating structural systems under seismic excitations. *Technical Report No. TB 177*, The John A. Blume Earthquake Engineering Center, Stanford Univ., Stanford, CA.
- [23] Idota H, Guan L, Yamazaki K (2009): Statistical correlation of steel members for system reliability analysis. *Proceedings of the 9<sup>th</sup> International Conference on Structural Safety and Reliability (ICOSSAR)*, Osaka, Japan.
- [24] Hancock J, Watson-Lamprey J, Abrahamson N, Bommer J, Markatis A, McCoy E, Mendis R, (2006) An improved method of matching response spectra of recorded earthquake ground motion using wavelets, *Journal of Earthquake Engineering*, **10**(Special Issue 1): 67-89.
- [25] Diaz SA, Pujades LG, Barbat AH, Félix JL (2015) Efecto de la direccionalidad en la amenaza sísmica de la Ciudad de México. *20<sup>th</sup> Congreso Nacional de Ingeniería Sísmica México*. Acapulco, Guerrero. ISSN: 2448-5721.
- [26] Satyarno I (2000): Adaptive pushover analysis for the seismic assessment of older reinforced concrete buildings. *Doctoral Thesis*, Department of civil engineering, University of Canterbury. New Zealand.
- [27] Park YJ, Ang AH-S, Wen YK (1985): Seismic damage analysis of reinforced concrete buildings. *Journal of Structural Engineering*, 111, 740–757.